GENETICS

Supporting Information
http://www.genetics.org/content/suppl/2011/05/30/genetics.111.128231.DC1

Cell Polarity in *Saccharomyces cerevisiae* Depends on Proper Localization of the Bud9 Landmark Protein by the EKC/KEOPS Complex

Yu Kato, Hiroshi Kawasaki, Yoshifumi Ohyama, Takashi Morishita, Hiroshi Iwasaki, Tetsuro Kokubo, and Hisashi Hirano

DOI: 10.1534/genetics.111.128231

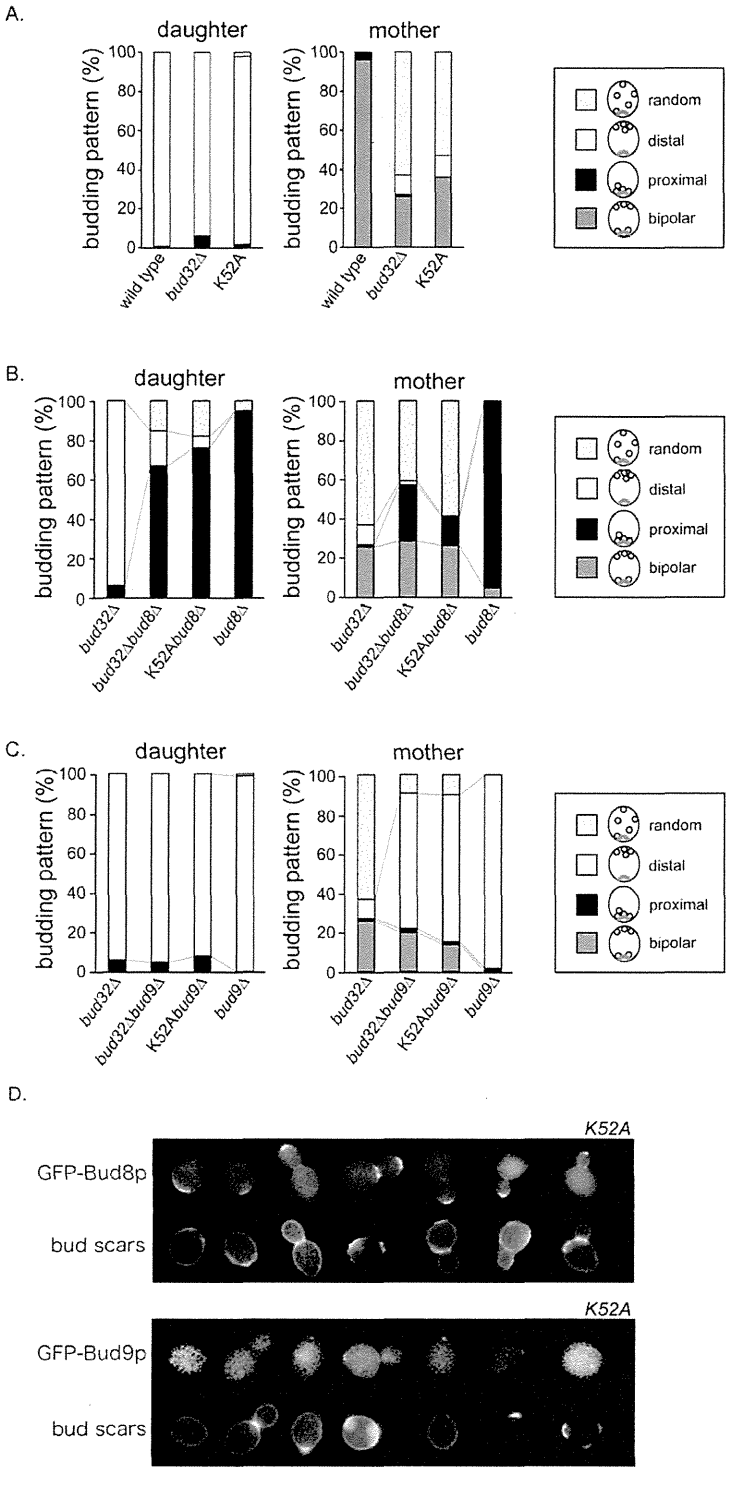

Figure S1 Phenotype of the kinase dead mutant (*bud32-K52*). (A) Budding patterns of the kinase dead mutant. Strains used were diploid BY4743, the *bud32*Δ (CCY003), the *bud32-K52A* (CCY056). (B) Budding pattern of cells with *BUD8* deletion in the kinse dead mutant backgrounds. Diploid strains used were the *bud32*Δ (CCY003), *bud32*Δ*bud8*Δ (CCY026), *K52Abud8*Δ (CCY058) and *bud8*Δ (CCY011). (C) Budding pattern of cells with *BUD9* deletion in the kinse dead mutant backgrounds. Diploid strains used were the *bud32*Δ (CCY003), *bud32*Δ*bud9*Δ (CCY029), *K52Abud9*Δ (CCY060) and *bud9*Δ (CCY013). Budding positions are classified as in the budding pattern of diploid cells

in Figure 1A. At least 150 cells were scored for each bud scar pattern from both daughter and mother cells; the percentages are indicated. The black, white, and dotted boxes indicate daughter cells with bud at only the proximal pole, only the distal pole, or the random site, respectively. The gray, black, white, and dotted boxes indicate mother cells with buds at two poles, only the proximal pole, only the distal pole, or the random site, respectively. (D) Localization of GFP-Bud8p and GFP-Bud9p in the kinase dead mutant. The *bud32-K52A* (CCY065) mutant expressing full-length GFP-Bud8p and GFP-Bud9p from its own promoter in pYC14 or pYC06, respectively, was grown for 12-16h at 25°C in synthetic complete (SC)–Leu or –Ura liquid medium, stained with calcofluor white, and then suspended in water for observation. GFP-Bud8p/GFP-Bud9p and bud scars were observed with a fluorescence microscope with GFP and UV filter sets, respectively.

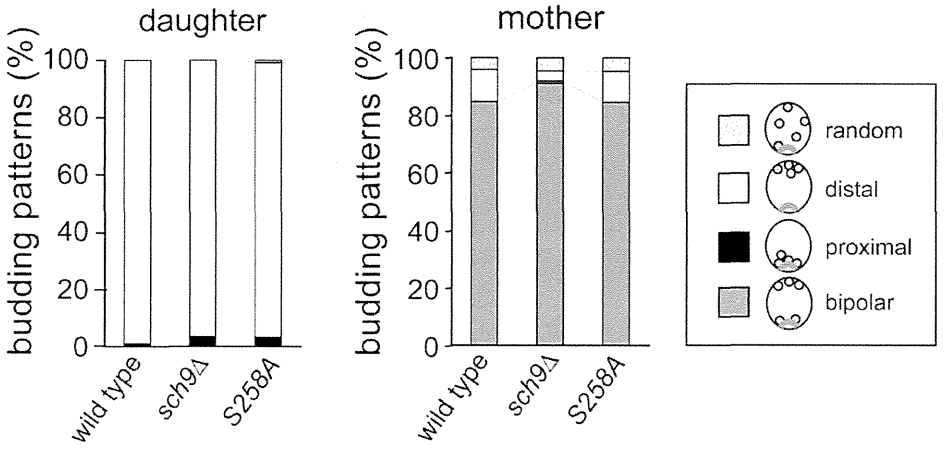

Figure S2 Budding patterns of *bud32-S258A* and *sch9*D mutant. Strains used were diploid BY4743, *sch9*Δ (CCY070) and *bud32-S258A* (CCY068). Budding positions are classified as in the budding pattern of diploid cells in Figure 1A. At least 150 cells were scored for each bud scar pattern from both daughter and mother cells; the percentages are indicated. The black, white, and dotted boxes indicate daughter cells with bud at only the proximal pole, only the distal pole, or the random site, respectively. The gray, black, white, and dotted boxes indicate mother cells with buds at two poles, only the proximal pole, only the distal pole, or the random site, respectively.

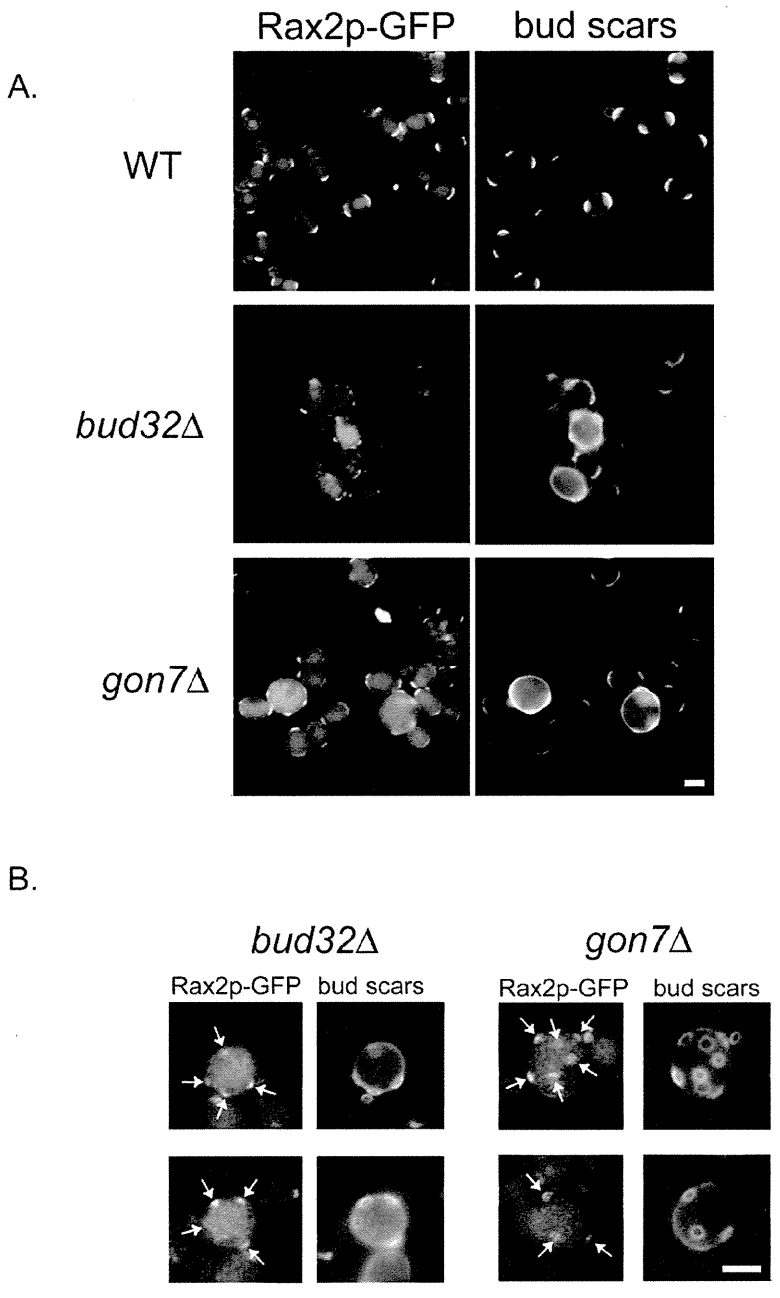

Figure S3 Localization of Rax2p-GFP in *bud32*Δ and *gon7*Δ mutants. (A) Diploid *bud32*Δ (CCY036) and *gon7*Δ (CCY041) expressing Rax2p-GFP from their own promoter at their chromosomal locus were grown overnight to log phase in YPD liquid medium, stained with calcofluor white, and then suspended in water for observation. Rax2p-GFP and bud scars were observed with a fluorescence microscope using GFP and UV filter sets, respectively. Scale bar indicates 5 μm. (B) Bud scars at the equatorial position of random budding sites were also marked by Rax2p-GFP in diploid *bud32*Δ (CCY036) and *gon7*Δ (CCY041) mutants. The arrows indicate Rax2p-GFP localization at random positions. Scale bar indicates 5 μm.

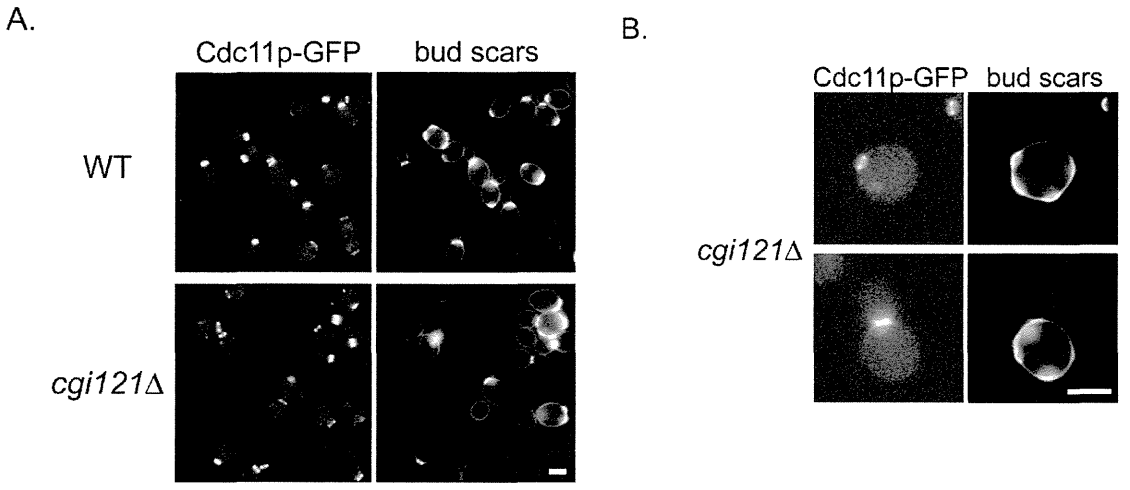

Figure S4 Effect on the licalization of a septin component, Cdc11p-GFP. (A) Localization of Cdc11p-GFP in *cgi121*Δ mutants and wild type cells. Diploid wild-type (CCY073) and *cgi121*Δ (CCY075) mutant cells expressing Cdc11p-GFP at its chromosomal loci were grown overnight to log phase in YPD liquid medium and the suspended in water for observation. Cdc11p-GFP and bud scars were observed with fluorescence microscope using a GFP and UV filter sets, respectively. Scale bar indicates 5 μm. (B) The septin ring is formed in the mutant cells at the equatorial position. Scale bar indicates 5 μm.

Table S1 Strains used in this study

Strains	Relevant genotype[a]	Source
BY4741	a his3-Δ1 leu2-Δ1 ura3-Δ0 met15-Δ1	our stock
BY4742	α his3-Δ1 leu2-Δ1 ura3-Δ0 lys-Δ0	our stock
BY4743	a/α his3-Δ1/his3-Δ1 leu2-Δ1/leu2-Δ1 ura3-Δ0/ura3-Δ0 met15-Δ1/lys-Δ0	our stock
CCY001	a his3-Δ1 leu2-Δ1 ura3-Δ0 met15-Δ1 bud32Δ::kanMX6	EUROSCARF
CCY002	α his3-Δ1 leu2-Δ1 ura3-Δ0 lys-Δ0 bud32Δ::kanMX6	Open Biosystems, Inc.
CCY003	a/α his3-Δ1/his3-Δ1 leu2-Δ1/leu2-Δ1 ura3-Δ0/ura3-Δ0 met15-Δ1/met15-Δ1 bud32Δ::kanMX6/bud32Δ::kanMX6	Open Biosystems, Inc.
CCY004	a his3-Δ1 leu2-Δ1 ura3-Δ0 met15-Δ1 cgi121Δ::kanMX6	EUROSCARF
CCY005	α his3-Δ1 leu2-Δ1 ura3-Δ0 lys-Δ0 cgi121Δ::kanMX6	Open Biosystems, Inc.
CCY006	a/α his3-Δ1/his3-Δ1 leu2-Δ1/leu2-Δ1 ura3-Δ0/ura3-Δ0 met15-Δ1/met15-Δ1 cgi121Δ::kanMX6/cgi121Δ::kanMX	Open Biosystems, Inc.
CCY007	a his3-Δ1 leu2-Δ1 ura3-Δ0 met15-Δ1 gon7Δ::kanMX6	EUROSCARF
CCY008	α his3-Δ1 leu2-Δ1 ura3-Δ0 lys-Δ0 gon7Δ::kanMX6	Open Biosystems, Inc.
CCY009	a/α his3-Δ1/his3-Δ1 leu2-Δ1/leu2-Δ1 ura3–Δ0/ura3-Δ0 met15-Δ1/met15-Δ1 gon7Δ::kanMX6/gon7Δ::kanMX6	Open Biosystems, Inc.
CCY010	a his3-Δ1 leu2-Δ1 ura3-Δ0 met15-Δ1 bud8Δ::kanMX6	EUROSCARF
CCY011	a/α his3-Δ1/his3-Δ1 leu2-Δ1/leu2-Δ1 ura3-Δ0/ura3-Δ0 met15-Δ1/met15-Δ1 bud8Δ::kanMX6/bud8Δ::kanMX6	a/α conversion from CCY010
CCY012	a his3-Δ1 leu2-Δ1 ura3-Δ0 met15-Δ1 bud9Δ::kanMX6	EUROSCARF
CCY013	a/α his3-Δ1/his3-Δ1 leu2-Δ1/leu2-Δ1 ura3-Δ0/ura3-Δ0 met15-Δ1/met15-Δ1 bud9Δ::kanMX6/bud9Δ::kanMX6	a/α conversion from CCY012
CCY014	a his3-Δ1 leu2-Δ1 ura3-Δ0 met15-Δ1 bud32Δ::kanMX6 cgi121Δ::kanMX6	segregant from CCY001xCCY005
CCY015	a his3-Δ1 leu2-Δ1 ura3-Δ0 met15-Δ1 bud32Δ::kanMX6 gon7Δ::URA3	see textb

CCY016	a his3-Δ1 leu2-Δ1 ura3-Δ0 met15-Δ1 cgi121Δ::kanMX6 gon7Δ::URA3	see textb
CCY017	a/α his3-Δ1/his3-Δ1 leu2-Δ1/leu2-Δ1 ura3-Δ0/ura3-Δ0 met15-Δ1/met15-Δ1 bud32Δ::kanMX6/bud32Δ::kanMX6 cgi121Δ::kanMX6/cgi121Δ::kanMX6	a/α conversion from CCY014
CCY018	a/α his3-Δ1/his3-Δ1 leu2-Δ1/leu2-Δ1 ura3-Δ0/ura3-Δ0 met15-Δ1/met15-Δ1 bud32Δ::kanMX6/bud32Δ::kanMX6 gon7Δ::URA3/gon7Δ::URA3	a/α conversion from CCY015
CCY019	a/α his3-Δ1/his3-Δ1 leu2-Δ1/leu2-Δ1 ura3-Δ0/ura3-Δ0 met15-Δ1/met15-Δ1 cgi121Δ::kanMX6/cgi121Δ::kanMX6 gon7Δ::URA3/gon7Δ::URA3	a/α conversion from CCY016
CCY020	a his3-Δ1 leu2-Δ1 ura3-Δ0 met15-Δ1 bud8Δ::kanMX6 bud32Δ::kanMX6	segregant from CCY002xCCY010
CCY021	a his3-Δ1 leu2-Δ1 ura3-Δ0 met15-Δ1 bud8Δ::kanMX6 cgi121Δ::kanMX6	segregant from CCY005xCCY010
CCY022	a his3-Δ1 leu2-D1 ura3-Δ0 met15-Δ1 bud8Δ::kanMX6 gon7Δ::URA3	see textb
CCY023	a his3-Δ1 leu2-Δ1 ura3-Δ0 met15-Δ1 bud9Δ::kanMX6 bud32Δ::kanMX6	segregant from CCY002xCCY012
CCY024	a his3-Δ1 leu2-Δ1 ura3-Δ0 met15-Δ1 bud9Δ::kanMX6 cgi121Δ::kanMX6	segregant from CCY005xCCY012
CCY025	a his3-Δ1 leu2-Δ1 ura3-Δ0 met15-Δ1 bud9Δ::kanMX6 gon7Δ::URA3	see textb
CCY026	a/α his3-Δ1/his3-Δ1 leu2-Δ1/leu2-Δ1 ura3-Δ0/ura3-Δ0 met15-Δ1/met15-Δ1 bud8Δ::kanMX6/bud8Δ::kanMX6 bud32Δ::kanMX6/bud32Δ::kanMX6	a/α conversion from CCY020
CCY027	a/α his3-Δ1/his3-Δ1 leu2-Δ1/leu2-Δ1 ura3-Δ0/ura3-Δ0 met15-Δ1/met15-Δ1 bud8Δ::kanMX6/bud8Δ::kanMX6 cgi121Δ::kanMX6/cgi121Δ::kanMX6	a/α conversion from CCY021
CCY028	a/α his3-Δ1/his3-Δ1 leu2-Δ1/leu2-Δ1 ura3-Δ0/ura3-Δ0 met15-Δ1/met15-Δ1 bud8Δ::kanMX6/bud8Δ::kanMX6 gon7Δ::URA3/gon7Δ::URA3	a/α conversion from CCY022
CCY029	a/α his3-Δ1/his3-Δ1 leu2-Δ1/leu2-Δ1 ura3-Δ0/ura3-Δ0 met15-Δ1/met15-Δ1 bud9Δ::kanMX6/bud9Δ::kanMX6 bud32Δ::kanMX6/bud32Δ::kanMX6	a/α conversion from CCY023
CCY030	a/α his3-Δ1/his3-Δ1 leu2-Δ1/leu2-Δ1 ura3-Δ0/ura3-Δ0 met15-Δ1/met15-Δ1 bud9Δ::kanMX6/bud9Δ::kanMX6 cgi121Δ::kanMX6/cgi121Δ::kanMX6	a/α conversion from CCY024
CCY031	a/α his3-Δ1/his3-Δ1 leu2-Δ1/leu2-Δ1 ura3-Δ0/ura3-Δ0 met15-Δ1/met15-Δ1 bud9Δ::kanMX6/bud9Δ::kanMX6 gon7Δ::URA3/gon7Δ::URA3	a/α conversion from CCY025

CCY032	a his3-Δ1 leu2-Δ1 ura3-Δ0 met15-Δ1 RAX2-GFP-kanMX6::RAX2	see text
CCY033	α his3-Δ1 leu2-Δ1 ura3-Δ0 lys-Δ0 RAX2-GFPkanMX6::RAX2	see text
CCY034	a/α his3-Δ1/his3-Δ1 leu2-Δ1/leu2-Δ1 ura3-Δ0/ura3-Δ0 met15-Δ1/lys-Δ0 RAX2-GFP-kanMX6::RAX2/RAX2-GFP-kanMX6::RAX2	mating of CCY032 and CCY033
CCY035	a his3-Δ1 leu2-Δ1 ura3-Δ0 met15-Δ1 RAX2-GFP-kanMX6::RAX2 bud32Δ::kanMX6	segregant from CCY002xCCY032
CCY036	a/α his3-Δ1/his3-Δ1 leu2-Δ1/leu2-Δ1 ura3-Δ0/ura3-Δ0 met15-Δ1/met15-Δ1 RAX2-GFP-kanMX6::RAX2/RAX2-GFP-kanMX6::RAX2bud32Δ::kanMX6/bud32Δ::kanMX6	a/α conversion from CCY035
CCY037	a his3-Δ1 leu2-Δ1 ura3-Δ0 met15-Δ1 RAX2-GFP-kanMX6::RAX2 cgi121Δ::kanMX6	segregant from CCY005xCCY032
CCY038	a/α his3-Δ1/his3-Δ1 leu2-Δ1/leu2-Δ1 ura3-Δ0/ura3-Δ0 met15-Δ1/met15-Δ1 RAX2-GFP-kanMX6::RAX2/RAX2-GFP-kanMX6::RAX2 cgi121Δ::kanMX6/cgi121Δ::kanMX6	a/α conversion from CCY037
CCY039	a/α his3-Δ1/his3-Δ1 leu2-Δ1/leu2-Δ1 ura3-Δ0/ura3-Δ0 met15-Δ1/lys-Δ0 RAX2-GFP-kanMX6::RAX2/RAX2-GFP-kanMX6::RAX2 gon7Δ::hisMX6/GON7	see text
CCY040	a his3-Δ1 leu2-Δ1 ura3-Δ0 met15-Δ1 RAX2-GFP-kanMX6::RAX2 gon7Δ::hisMX6	segregant from CCY039
CCY041	a/α his3-Δ1/his3-Δ1 leu2-Δ1/leu2-Δ1 ura3-Δ0/ura3-Δ0 met15-Δ1/met1 RAX2-GFP-kanMX6::RAX2/ RAX2-GFP-kanMX6::RAX2 gon7Δ::hisMX6/gon7Δ::hisMX6	a/α conversion from CCY040
CCY042	a his3-Δ1 leu2-Δ1 ura3-Δ0 met15-Δ1 rax2Δ::kanMX6	EUROSCARF
CCY043	α his3-Δ1 leu2-Δ1 ura3-Δ0 lys-Δ0 rax2Δ::kanMX6	Open Biosystems, Inc.
CCY044	a/α his3-Δ1/his3-Δ1 leu2-Δ1/leu2-Δ1 ura3-Δ0/ura3-Δ0 met15-Δ1/lys-Δ0 rax2Δ::kanMX6/rax2Δ::kanMX6	mating of CCY042 and CCY043
CCY045	α his3-Δ1 leu2-Δ1 ura3-Δ0 lys-Δ0 rax2Δ::kanMX6 bud32Δ::kanMX6	segregant from CCY002xCCY042
CCY046	a/α his3-Δ1/his3-Δ1 leu2-Δ1/leu2-Δ1 ura3-Δ0/ura3-Δ0 lys-Δ0/lys-Δ0 rax2Δ::kanMX6/rax2Δ::kanMX6 bud32Δ::kanMX6/bud32Δ::kanMX6	a/α conversion from CCY045
CCY047	α his3-Δ1 leu2-Δ1 ura3-Δ0 lys-Δ0 rax2Δ::kanMX6 cgi121Δ::kanMX6	segregant from CCY005xCCY042
CCY048	a/α his3-Δ1/his3-Δ1 leu2−Δ1/leu2-Δ1 ura3-Δ0/ura3-Δ0 lys-Δ0/lys-Δ0 rax2Δ::kanMX6/rax2Δ::kanMX6 cgi121Δ::kanMX6/cgi121Δ::kanMX6	a/α conversion from CCY047

CCY049	a/ α his3-Δ1/his3-Δ1 leu2-Δ1/leu2-Δ1 ura3-Δ0/ura3-Δ0 met15-Δ1/met15-Δ1 rax2Δ::kanMX6/rax2Δ::kanMX6 gon7Δ::hisMX6/GON7	see text
CCY050	a his3-Δ1 leu2-Δ1 ura3-Δ0 met15-Δ1 rax2Δ::kanMX6 gon7Δ::hisMX6	segregant from CCY049
CCY051	a/ α his3-Δ1/his3-Δ1 leu2-Δ1/leu2-Δ1 ura3-Δ0/ura3-Δ0 met15-Δ1/met15-Δ1 rax2Δ::kanMX6/rax2Δ::kanMX6 gon7Δ::hisMX6/gon7Δ::hisMX6	a/ α conversion from CCY050
CCY052	a his3-Δ1 leu2-Δ1 ura3-Δ0 met15-Δ1 BUD32-GFP::BUD32	see text
CCY053	a/ α his3-Δ1/his3-Δ1 leu2-Δ1/leu2-Δ1 ura3-Δ0/ura3-Δ0 met15-Δ1/met15-Δ1 BUD32-GFP::BUD32/BUD32-GFP::BUD32	a/ α conversion from CCY052
CCY054	a his3-Δ1 leu2-Δ1 ura3-Δ0 met15-Δ1 BUD32(K52A)-GFP::BUD32	see text
CCY055	α his3-Δ1 leu2-Δ1 ura3-Δ0 lys-Δ0 BUD32(K52A)-GFP::BUD32	see text
CCY056	a/ α his3-Δ1/his3-Δ1 leu2-Δ1/leu2-Δ1 ura3-Δ0/ura3-Δ0 met15-Δ1/ lys-Δ0 BUD32(K52A)-GFP::BUD32/BUD32(K52A)-GFP::BUD32	mating of CCY054 and CCY055
CCY057	a his3-Δ1 leu2-Δ1 ura3-Δ0 met15-Δ1 BUD32(K52A)-GFP::BUD32 bud8Δ::kanMX6	segregant from CCY10xCCY055
CCY058	a/ α his3-Δ1/his3-Δ1 leu2-Δ1/leu2-Δ1 ura3-Δ0/ura3-Δ0 met15-Δ1/met15-Δ1 BUD32(K52A)-GFP::BUD32/ BUD32(K52A)-GFP::BUD32 bud8Δ::kanMX6/ bud8Δ::kanMX6	a/ α conversion from CCY057
CCY059	a his3-Δ1 leu2-Δ1 ura3-Δ0 met15-Δ1 BUD32(K52A)-GFP::BUD32 bud9Δ::kanMX6	segregant from CCY12xCCY055
CCY060	a/ α his3-Δ1/his3-Δ1 leu2-Δ1/leu2-Δ1 ura3-Δ0/ura3-Δ0 met15-Δ1/met15-Δ1 BUD32(K52A)-GFP::BUD32/ BUD32(K52A)-GFP::BUD32 bud9Δ::kanMX6/ bud9Δ::kanMX6	a/ α conversion from CCY059
CCY062	a his3-Δ1 leu2-Δ1 ura3-Δ0 met15-Δ1 BUD32-13myc:BUD32	see text
CCY063	a/ α his3-Δ1/his3-Δ1 leu2-Δ1/leu2-Δ1 ura3-Δ0/ura3-Δ0 met15-Δ1/met15-Δ1 BUD32-13myc:BUD32/ BUD32-13myc:BUD32	a/ α conversion from CCY062
CCY064	a his3-Δ1 leu2-Δ1 ura3-Δ0 met15-Δ1 BUD32(K52A):BUD32	see text
CCY065	a his3-Δ1 leu2-Δ1 ura3-Δ0 met15-Δ1 BUD32(K52A)-13myc:BUD32(K52A)	see text
CCY066	a/ α his3-Δ1/his3-Δ1 leu2-Δ1/leu2-Δ1 ura3-Δ0/ura3-Δ0 met15-Δ1/met15-Δ1 BUD32(K52A)-13myc:BUD32(K52A)/ BUD32(K52A)-13myc:BUD32(K52A)	a/ α conversion from CCY065

CCY067	a his3-Δ1 leu2-Δ1 ura3-Δ0 met15-Δ1 BUD32 (S258A)-GFP::BUD32	see text
CCY068	a/α his3-Δ1/his3-Δ1 leu2-Δ1/leu2-Δ1 ura3-Δ0/ura3-Δ0 met15-Δ1/met15-Δ1 BUD32(S258A)-GFP:BUD32/BUD32(S258A)-GFP::BUD32	a/α conversion from CCY067
CCY069	a his3-Δ1 leu2-Δ1 ura3-Δ0 met15-Δ1 sch9Δ::kanMX6	Open Biosystems, Inc.
CCY070	a/α his3-Δ1/his3-Δ1 leu2-Δ1/leu2-Δ1 ura3-Δ0/ura3-Δ0 met15-Δ1/met15-Δ1 sch9Δ::kanMX6/sch9Δ::kanMX6	a/α conversion from CCY069
CCY071	a his3-Δ1 leu2-Δ1 ura3-Δ0 met15-Δ1 CDC11-GFP-kanMX6::CDC11	see text
CCY072	α his3-Δ1 leu2-Δ1 ura3-Δ0 lys-Δ0 CDC11-GFP-kanMX6::CDC11	see text
CCY073	a/α his3-Δ1/his3-Δ1 leu2-Δ1/leu2-Δ1 ura3-Δ0/ura3-Δ0 met15-Δ1/lys-Δ0 CDC11-GFP-kanMX6::CDC11/CDC11-GFP-kanMX6::CDC11	mating of CCY071 and CCY072
CCY074	a his3-Δ1 leu2-Δ1 ura3-Δ0 met15-Δ1 CDC11-GFP-kanMX6::CDC11 cgi121Δ::kanMX6/cgi121Δ::kanMX	segregant of CCY071xCCY005
CCY075	a/α his3-Δ1/his3-Δ1 leu2-Δ1/leu2-Δ1 ura3-Δ0/ura3-Δ0 met15-Δ1/met15-Δ1 CDC11-GFP-kanMX6::CDC11/CDC11-GFP-kanMX6::CDC11 cgi121Δ::kanMX6/cgi121Δ::kanMX6	a/α conversion from CCY074

624

a All strains are congenic to BY4743.

b The strain was generated by a precise replacement of the GON7 open reading frame by URA3.

Table S2 Plasmids used in this study

Plasmid	Description	Source
pBluescript (SK-)	Ampicillin (cloning)	Stratagene
pFA6a-kanMX	Kanamycin (integrative)	Longtine *et al.* (1998)
pFA6a-GFP^{S65T}-kanMX	Kanamycin (integrative)	Longtine *et al.* (1998)
pFA6a-13Myc-kanMX	Kanamycin (integrative)	Longtine *et al.* (1998)
pRS306	*URA3* (integrative)	Sikorski and Hieter (1989)
pRS425	*LEU2* (high copy)	Christianson *et al.* (1992)
pRS426	*URA3* (high copy)	Christianson *et al.* (1992)
pTM55	*Xho*I/*Sal*I fragment containing triple FLAG tag	our stock
pYC01	3138 bps *Xho*I/*Spe*I fragment containing *BUD8* gene in pRS425	see text
pYC02	3245 bps *Xho*I/*Spe*I fragment containing *BUD9* gene in pRS426	see text
pYC03	*Mlu*I restriction site at just downstream of start codon on *BUD8* in pYC01	see text
pYC04	*Mlu*I restriction site at just downstream of start codon on *BUD9* in pYC02	see text
pYC05	*Mlu*I fragments containing *GFP* sequence in pBluescript (SK-)	see text
pYC06	*GFP-BUD9* in pRS426	Kato *et al.* (2009)
pYC07	1460 bps fragment containing *GON7* gene in pBluescript (SK-)	see text
pYC08	1089 bps fragment without *GON7* gene in pBluescript (SK-)	see text
pYC09	*GON7*:: *URA3* in pBluescript (SK-)	see text
pYC10	*FLAG$_6$-BUD9* in pRS426	see text
pYC11	2094 bps *Spe*I/*Xho*I fragment containing *BUD32* in pBluescript (SK-)	see text
pYC12	*Mlu*I restriction site at just upstream of stop codon on *BUD32* in pYC11	see text
pYC13	*BUD32 (K52A)* in pBluescript (SK-)	see text
pYC14	*GFP-BUD8* in pRS425	Kato *et al.* (2009)
pYC15	*BUD32 (S258A)* in pBluescript (SK-)	see text
pYC16	*BUD32 (K52A)* in pRS306	see text
pYC17	*BUD32-GFP* in pBluescript (SK-)	see text
pYC18	*BUD32 (K52A)-GFP* in pBluescript (SK-)	see text
pYC19	*BUD32 (S258A)-GFP* in pBluescript (SK-)	see text
pYC20	*BUD32-GFP* in pRS306	see text

pYC21	*BUD32 (K52A)-GFP* in pRS306	see text
pCY22	*BUD32 (S258A)-GFP* in pRS306	see text

[a]The GFP sequences encode *GFP* with the S65T substitution.

626

Table S3 **Primers used in this study**

Primer	sequences
T7 promoter	TAATACGACTCACTATAGGG
M13 reverse	CAGGAAACAGCTATGAC
BUD8a	AAAAAA***CTCGAG***ACTTCAACCACCTTCA
BUD8b	AAAAAA***ACTAGT***AGAAGTACGGTTACAAGACT
BUD8c	***ACGCGT***ATACAATCAGACGAAG
BUD8d	CATACTTCATGTAGAATCG
BUD9a	AAAAAA***CTCGAG***CACAAGAACATTTCTG
BUD9b	AAAAAA***ACTAGT***CTCTATCGTACTCCTC
BUD9c	***ACGCGT***ACGAAAATAACCAGAG
BUD9d	CATTTCATAGGATGAAGAATG
BUD32a	AAAAAAACTAGTAAACGTCGATTTTACCAG
BUD32b	AAAAAACTCGAGGATAGTCATTCTTTCC
BUD32c	AAGAGAAGTATGCTAGGAACGCGTTAATATAAATGCTAGCG
BUD32d	GAGAAGTATGCTAGGAACGCGTTATAAATGCTAGCGTA
BUD32e	GCATATAGGCCACCAAAGCGTTATAG
BUD32f	GATAATATACTTTTGATGAGAATCCTTTGC
BUD32g	GCTATGCTAGGATAATATAAATGCTAGCG
BUD32h	TCTCTTACGACCACGCAACCTG
BUD32i	AAAAGATTCGAAGAGGTCAGGTTGCGTGGTCGTAAGAAGTATGCTAGGAGCAGGTCGA
BUD32j	TGTGCAGCGATATACAGGCAGTACGCTAGCATTTATATTAGAATTCGAGCTCGTTTAAAC
GFPa	AAAAAAACGCGTGGGTTAATTAACAGTAAA
GFPb	A***ACGCGT***TTTGTATAGTTCATCCATGCC
GFPc	A***GATATC***GGGTTAATTAACAGTAAAGGAG
GFPd	A***GATATC***TTTGTATAGTTCATCCATGCCATG
GON7a	AAAACTAGTAAATAGCGATTCTTCATCGTGAATG
GON7b	AAACTCGAGTAACGGTCATTTGTTTTAACACAG
GON7c	GCAACGATATGTAGCGCTAGAG
GON7d	***ACGCGT***TGAGATATTAGGATAAGGTTC

GON7e	TATACAGCCGATAGTGCACTGGAACCTTATCCTAATATCTCACGGATCCCCGGTTAATT
GON7f	GACTCTTTTCTGTTTGTATATACACTCTCTAGCGCTACATATCGT
URA3a	AAAA***ACGCGT***AAGCTTTGGCACATCAATG
URA3b	AAAA***ACGCGT***ACCGTTGTTATCAGAAATTC
RAX2a	AGAATGAAATGCTTGATACCGTCCCACCCGAAAAACTTATGAAGTTTGTCCGGATCCCCGGGTTAATTAA
RAX2b	AGTGTTCATTATTTTAAGTAGTTATATATTATATAATACAACCCCGATTAGAATTCGAGCTCGTTTAAAC
CDC11a	ATTGAAGCCAGGTTGGAAAAAGAGGCGAAAATCAAACAGGAAGAACGGATCCCCGGGTTAATTAA
CDC11b	ATATAGAGAAAGAAGAAATAAGTGAGGAAGCCAAAAGCGGACGAATTCGAGCTCGTTTAAAC

The bold italics indicate restriction sites.

the FEBS Journal

Wild-type p53 enhances annexin IV gene expression in ovarian clear cell adenocarcinoma

Yusuke Masuishi[1,*], Noriaki Arakawa[1,*], Hiroshi Kawasaki[1], Etsuko Miyagi[2], Fumiki Hirahara[2] and Hisashi Hirano[1]

1 Department of Supramolecular Biology, Graduate School of Nanobioscience, Yokohama City University, Japan
2 Department of Obstetrics and Gynecology, Yokohama City University School of Medicine, Japan

Keywords
annexin IV; clear cell adenocarcinoma; ovarian cancer; p53; promoter

Correspondence
N. Arakawa or H. Hirano, Department of Supramolecular Biology Graduate School of Nanobioscience Yokohama City University, 1-7-29 Suehiro-cho, Tsurumi-ku, Yokohama 230-0045, Japan
Fax: +81 45 508 7667
Tel: +81 45 508 7247
E-mail: arakawa@yokohama-cu.ac.jp

*These authors contributed equally to this work

(Received 13 December 2010, revised 25 January 2011, accepted 21 February 2011)

doi:10.1111/j.1742-4658.2011.08059.x

The protein annexin IV (ANX4) is elevated specifically and characteristically in ovarian clear cell adenocarcinoma (CCA), a highly malignant histological subtype of epithelial ovarian cancer. On the basis of the hypothesis that the expression of *ANX4* in CCA is regulated by a unique transcription mechanism, we explored the *cis*-elements involved in CCA-specific ANX4 expression using a luciferase reporter. We compared the transcriptional activities of the region from −1534 to +1010 relative to the *ANX4* transcription start site in CCA and non-CCA-type cell lines, and found that two repeated binding motifs for the tumor suppressor protein, p53, in the first intron of *ANX4* were involved in CCA-specific transcriptional activity. Furthermore, chromatin immunoprecipitation showed that endogenous p53 bound to this site in CCA cell lines. Moreover, the use of short interference RNA to silence the *p53* gene decreased the transcriptional activity and mRNA expression of *ANX4* in CCA cell lines. Thus, the *ANX4* gene is, at least in part, regulated by p53 in CCA cells. Mutations in the *p53* gene were absent and levels of p53 target genes were higher in several CCA-derived cell lines. Although the expression of ANX4 is typically low in these non-CCA cell lines, ANX4 levels were elevated more than three-fold by the overexpression of wild-type but not mutant p53. Therefore, we conclude that the *ANX4* gene is a direct transcriptional target of p53, and its expression is enhanced by wild-type p53 in CCA cells.

Introduction

Epithelial ovarian carcinoma (EOC), which comprises the majority of ovarian cancers, is a leading cause of death among gynecological malignancies [1]. This disease is both morphologically and biologically heterogeneous, and can be divided into four major histological subtypes based on morphological criteria: serous, endometrioid, mucinous and clear cell carcinoma. Clear cell adenocarcinoma (CCA) is distinct histopathologically and clinically from the other EOC subtypes. Although the incidence of CCA is not high, patients with CCA have a markedly worse clinical prognosis than patients with other EOC subtypes. The recurrence of CCA is higher, even in the early stages, and the 3- and 5-year survival rates for CCA patients are significantly lower than for patients with other subtypes [2]. In addition, CCA shows a lower response to standard platinum-based chemotherapy. For these reasons, CCA is considered a highly malignant type of EOC.

CCA has several features that distinguish it from the other subtypes. The proliferative activity of CCA cells

Abbreviations
ANX4, annexin IV; CCA, clear cell adenocarcinoma; ChIP, chromatin immunoprecipitation; EOC, epithelial ovarian carcinoma; Mdm2, murine double minute 2; MMC, mitomycin C; NF-κB, nuclear factor-κB RNAi, RNA interference; siRNA, small interfering RNA.

is significantly lower than that of serous adenocarcinoma cells [3,4], which may help explain why CCA responds poorly to chemotherapy. Indeed, more patients are diagnosed during stage I of disease for CCA than for serous adenocarcinoma [5]. The tumor repressor gene *p53* is altered in 50–70% of advanced-stage EOC cells of all subtypes except CCA cells [6,7], in which it is only infrequently altered [8,9]. Furthermore, an immunohistochemical study of CCA tissue revealed a significant increase in the expression of the cyclin-dependent kinase inhibitor p21, a target of p53 [10]. Comprehensive gene expression profiling has revealed that the pattern of gene expression in CCA cells is clearly distinct from that of other EOC cells [11,12]. In particular, the annexin IV (annexin A4, ANX4) transcript is among a cluster of genes that are up-regulated in CCA cells. In addition, based on fluorescence 2D difference gel electrophoresis assays, it was previously shown [13] that ANX4 protein expression is markedly elevated in CCA-type cell lines and tissue compared to a mucinous adenocarcinoma-type cell line and tissue. Subsequently, Zhu *et al.* [14] compared proteomic patterns in 16 CCA and eight serous tissue samples, and also reported the up-regulation of ANX4 in all CCA tissues. More recently, in an immunohistological chemical study of more than 100 tissue samples of ovarian cancer patients, Kim *et al.* [15] found that more than 30 of the 43 CCA-type tissue samples were strongly positive for ANX4 compared to only five of the 62 serous-type samples. These findings suggest that the up-regulation of ANX4 is a unique characteristic of ovarian CCA.

ANX4 belongs to a ubiquitous family of calcium-dependent phospholipid-binding proteins. The function of the protein is assumed to differ between ANX isoforms [16]. Although little is known about the detailed physiological roles of ANX4, previous studies have reported the involvement of this protein in membrane permeability [17], exocytosis [18] and the regulation of ion channels [19]. Han *et al.* [20] and Kim *et al.* [15] reported that the level of ANX4 expression was associated with chemoresistance in human cancer cell lines. Therefore, it was suggested that ANX4 might constitute a novel therapeutic target for overcoming resistance to cancer chemotherapy in patients with ovarian CCA.

The elucidation of the molecular mechanisms regulating CCA-specific ANX4 expression may lead to a better understanding of the molecular biology unique to CCA cells, which is important for overcoming the malignancy of this disease. However, the mechanisms regulating the transcription of the *ANX4* gene have not been elucidated. In the present study, we characterized the flanking region of the transcription start site for *ANX4* and identified an intronic enhancer essential to the up-regulation of *ANX4* expression in CCA cells. We also found that the wild-type p53 protein binds to this region and acts as a positive regulator of *ANX4* gene expression in ovarian CCA.

Results

CCA-specific expression of ANX4

We previously found (using 2D difference gel electrophoresis analysis) that the amount of ANX4 was significantly higher in CCA than non-CCA cell lines and tissues [13]. We confirmed this finding by western blotting and real-time RT-PCR analyses using cell lines originating from CCA, OVTOKO and OVISE cultured cell lines, as well as the mucinous type of EOC, MCAS. ANX4 was detected strongly in OVTOKO and OVISE cells but not in MCAS cells (Fig. 1A). In the real-time RT-PCR experiment, the expression level of ANX4 mRNA was nine- and four-fold higher in OVTOKO and OVISE cells, respectively, than in

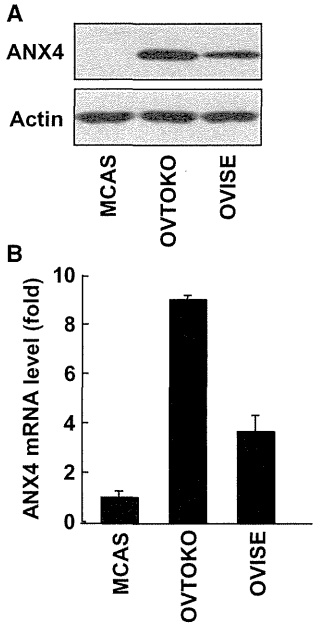

Fig. 1. ANX4 is up-regulated in CCA cell lines. Protein and RNA were extracted from two CCA (OVTOKO and OVISE) cells lines and one non-CCA (MCAS) cell line, and then ANX4 protein (A) and mRNA (B) levels were compared by western blotting and real-time RT-PCR analyses, respectively. Actin was included as a loading control. The values were normalized to the level of 18S ribosomal RNA expression in each sample. Bars represent the mean ± SE of three experiments.

MCAS cells (Fig. 1B). These results indicate that the expression level of ANX4 is increased in CCA cell lines compared to non-CCA cell lines, as demonstrated previously [13,15], and that ANX4 expression is controlled at the level of transcription. To determine the transcriptional factor responsible for these different expression levels of ANX4, we performed promoter/enhancer analysis of the *ANX4* gene using these three cell lines.

Determination of the 5′-end of the ANX4 mRNA

To determine the 5′-end of ANX4 mRNA, 5′-RACE analysis was performed using RNA isolated from MCAS, OVTOKO and OVISE cultured cell lines. Single DNA bands of the same size (170 bp) were detected for each cell line by agarose gel electrophoresis of the 5′-RACE products (Fig. 2A). Sequence analyses verified that each band had the same sequence, corresponding to the first through third exons of the ANX4 cDNA reported in the GenBank database (NM_001153.2), although the 5′-end identified in the present study was located upstream of the 5′-end reported in the database (Fig. 2B). We regarded the 5′-end determined by our 5′-RACE analysis as a putative transcription start site (+1) of *ANX4*.

The +180 region is essential for CCA-specific transcriptional activity of ANX4

To identify the *cis*-elements essential for CCA-specific expression of *ANX4*, we first isolated the region from −1534 to +1010 relative to the transcriptional start site and inserted it into a luciferase reporter vector (−1534/+1010 luc). Consensus TATA-box sequences were not found in the predicted positions of this region, although the region from −586 to +402 was identified as a CpG island (GC contents, 68%) using the software CPG ISLAND RESEARCHER (http://cpgislands.usc.edu/). The modified −1534/+1010 luc vector was

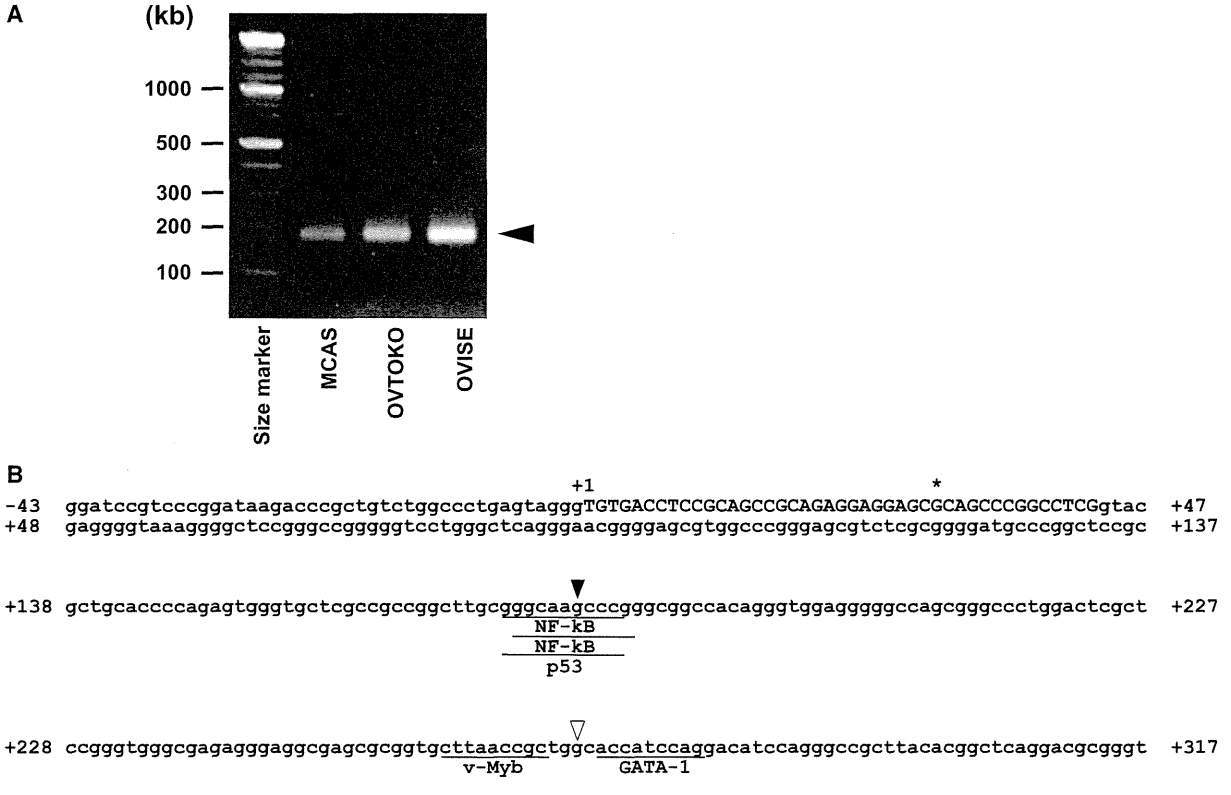

Fig. 2. The 5′-end of the *ANX4* gene. To determine the transcriptional start site of *ANX4* in EOC cells, the 5′-end of ANX4 mRNA was investigated by 5′-RACE analysis. (A) Agarose gel electrophoresis of PCR products from the 5′-RACE procedure. The arrowhead indicates the bands detected in three cell lines by 5′-RACE. (B) The nucleotide sequence of the flanking region of the *ANX4* transcription start site and putative transcription factor-binding sites within this region. Uppercase letters indicate the first exon of *ANX4*. The asterisk and +1 show the 5′-ends reported in the GenBank database (NM_001153.2) and identified newly in the present study, respectively. The putative binding sequences for the representative transcription factors are underlined. The nucleotide positions at +180 and +270 are denoted by filled and unfilled triangles, respectively.

transfected into MCAS, OVTOKO and OVISE cells, and the transcriptional activity was determined by luciferase assay (Fig. 3A). The −1534/+1010 region demonstrated approximately nine- and four-fold higher levels of transcriptional activity in OVTOKO and OVISE cells, respectively, compared to MCAS cells. This result is very similar to the real-time RT-PCR data (Fig. 1B), suggesting that the −1534/+1010 region contains an element essential for CCA-specific expression of *ANX4*. Therefore, we constructed the various 5′- or 3′-deletion mutants of the modified −1534/+1010 luc vector, and measured the transcriptional activity of each mutant (Fig. 3A). Deletion of the 3′-downstream region (−42 to +1010) resulted in a marked decrease in luciferase activity in OVTOKO and OVISE cells, although no change occurred in MCAS cells. Further deletion of the 5′-upstream region from −181 decreased luciferase activity in all three cell lines. By contrast, the deletion of the 5′-upstream region from −43 alone also reduced luciferase activity in all three cell lines, although it did not completely diminish the higher activity seen in OVTOKO and OVISE cells. This CCA-preferential activity of the region between −43 and +1010 was removed by deleting the 3′-downstream region from +28. These results suggest that an element essential for CCA-specific expression of *ANX4* is present between +27 and +1010 in the downstream region of the transcription start site. To further focus on the region essential for CCA-specific gene expression, serial 3′-deletions were constructed and subjected to luciferase reporter analysis (Fig. 3B). Deletion from

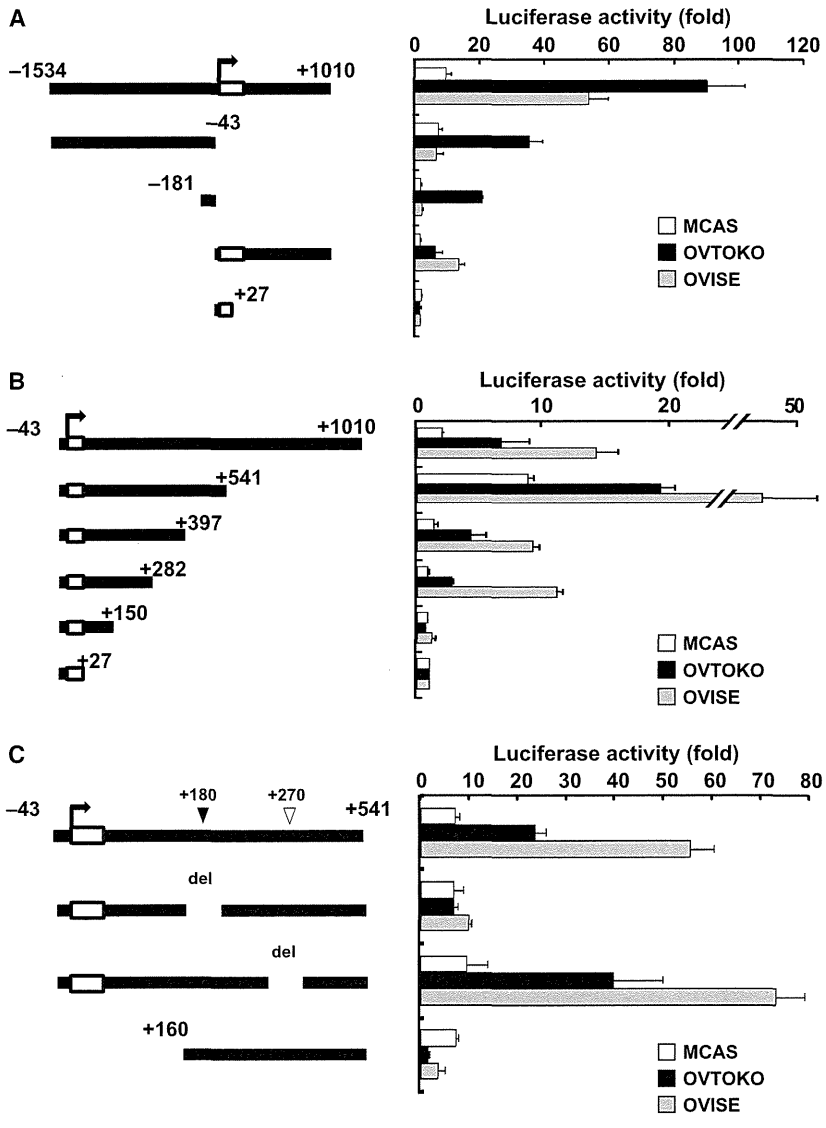

Fig. 3. CCA-specific transcriptional activity of *ANX4* depends on the +180 region in the first intron. The luciferase vector containing the flanking region of the *ANX4* transcriptional start site −1534/+1010 luc and its deletion mutants were introduced into OVTOKO, OVISE and MCAS cells, and the transcriptional activities were measured. Schematic diagrams of the *ANX4* promoter–luciferase plasmids are shown on the left, where the 5′- and 3′-ends are indicated relative to the transcription start site. (A) The 3′-downstream region of *ANX4* is essential for CCA-specific transcriptional activity. The luciferase activities of the full-length −1534/+1010 luc vector and the mutants with 5′-upstream or 3′-downstream deletions were compared. (B) The transcriptional activities of mutants with 3′-deletions in the region from −43 to +1010. (C) The effect of deleting the +180 or +270 regions on the transcriptional activities. Luciferase activity is expressed as the fold change relative to pGL3-basic vector activity in each cell. The β-galactosidase control vector was co-transfected as an internal control. Schematic diagrams of the *ANX4* promoter–luciferase plasmids are shown on the left, where the location of the 5′- and 3′-ends are indicated relative to the transcription start site. Bars represent the mean ± SE of at least three experiments.

+1010 up to +541, or from +541 to +397, resulted in marked changes in luciferase activity in all three cell lines. This suggests that the binding sites of both negative and positive regulatory transcription factors are contained in these two regions, although their role in ANX4 transcription is not specific to CCA cells. By contrast, the deletion of +282 to +150 decreased luciferase activity in OVTOKO and OVISE cells without altering activity in MCAS cells, suggesting that this region contains an element involved in CCA-specific expression of *ANX4*. In this region, the presence of putative transcription factor-binding sites was revealed by sequence analysis with the software TFSEARCH (http://www.cbrc.jp/research/db/TFSEARCH.html) and MOTIF (http://motif.genome.jp/) searching protein and nucleic acid sequence motifs. The nuclear factor (NF)-κB and p53-binding sites were found at position +180, and the GATA-binding site was found at position +270 (Fig. 2B). To determine which site was involved in CCA-specific *ANX4* expression, reporter analyses were performed using a luciferase construct containing the region −43 to +541 (−43/+541 luc) and mutants of this construct with regions at either +180 or +270 deleted. As shown in Fig. 3C, deleting the +270 region did not change the transcriptional activity of the −43/+541 luc of any cell line, whereas deleting the +180 region markedly decreased transcriptional activity in OVTOKO and OVISE cells but not in MCAS cells. Furthermore, CCA-specific transcriptional activity conferred by the +180 region was diminished by deleting the region upstream of +160. Accordingly, the +180 region acts as a transcription enhancer essential for the up-regulation of *ANX4* in CCA cells.

ANX4 expression is regulated by p53 in CCA

Potential binding sites for p53 and NF-κB were found in the +180 region (Fig. 2B). To determine whether these proteins conferred CCA-specific transcriptional activation of *ANX4*, two kinds of mutation patterns at the +180 region were designed. Both mutations, +180 mutA (5′-GGCCAAGCGTA-3′) and +180 mutB (5′-GGGAAAGCCCC-3′), abolished the putative p53-binding site. In addition, +180 mutA also destroyed the putative binding sequence for NF-κB, whereas +180 mutB maintained the NF-κB-binding sequence (5′-GGRNNYCC-3′). As shown in Fig. 4a, both +180 mutA and +180 mutB markedly decreased the transcriptional activity of the −43/+541 luc vector in OVTOKO and OVISE cells. Mutations at the +180 region reduced the transcriptional activity of the −1534/+1010 luc vector by half in CCA cells. Similar results were observed in the other EOC cell lines. Mutations at the +180 region significantly reduced transcriptional activity of the −43/+541 luc vector in the CCA cell lines RMG-I and RMG-II compared to the non-CCA cell lines OVCAR-3 and RMUG-S (Fig. S1). These results suggest that the +180 region acts as a p53-binding site in CCA cells.

The p53 protein binds to two copies of the motif 5′-RRRCWWGYYY-3′, separated by a variable spacer of length 0–13 bp [21]. The p53-binding motif in the +180 region matched this sequence exactly. Three sites at +161, +172 and +196 contained sequences similar to the p53-binding motif, although each was an incomplete motif. To determine whether these act as other

Fig. 4. p53 is a direct regulator of the *ANX4* gene in CCA. (A) The effect of mutating the +180 region on transcriptional activity. Two mutation patterns were made in the putative binding sequences for NF-κB and p53. In +180 mutA, both binding sequences were disrupted. In +180 mutB, the p53-binding sequence was disrupted, whereas the NF-κB-binding sequence had 100% consensus. These mutations were introduced into the indicated luciferase vectors. The β-galactosidase control vector was co-transfected with the luciferase vectors to normalize transfection efficiency. $*P < 0.05$ and $**P < 0.01$ versus −1534/+1010 luc. (B) The effect of mutating p53-binding motifs around the +180 region. The p53-binding motif-like sequences around the +180 region in the −43/+541 luc reporter were mutated (+180 mutA, +161 mut, +172 mut and +196 mut). The mutants were transfected into OVISE cells, and transcriptional activities were measured via luciferase assays. (C) p53 bound to the *ANX4* gene. ChIP assay was performed with OVISE, OVTOKO and MCAS cells and antibodies against p53. Immunoprecipitation of p53 protein–DNA complexes was conducted with control IgG or anti-p53 antibody (DO-1) or without antibody (noAb). Total lysate was used as a control for PCR amplification (input). PCR was performed with gene-specific primers for p21 and ANX4. As a positive control, p53 binding was tested with p21 specific primers targeting the genomic region harboring the p53-responsive element. The results displayed are representative of the findings from three independent experiments. (D) The expression levels of p53 in cells transfected with Stealth™ siRNA. Cell lines were transfected with siRNA and grown for 72 h, and then p53 protein levels were determined by western blotting. Representative western blots of three experiments are shown. Actin was included as a loading control. (E) The CCA-specific transcriptional activities of −43/+541 luc were suppressed by introducing p53 siRNA. siRNA-transfected cells were incubated for 24 h in one well of a 24-well plate, and then transfected with the −43/+541 luc vector and grown in culture for 24 h. The pRL-TK vector was co-transfected with the luc vector used as an internal control. (F) siRNA-transfected cells were grown for 72 h, and then the mRNA levels of ANX4 were quantified by real-time RT-PCR. All luciferase activity is expressed as the fold change relative to pGL3-basic vector activity. Schematic diagrams of the *ANX4* promoter–luciferase plasmids are shown on the left, where the location of the 5′- and 3′-ends are indicated relative to the transcription start site (A, B and E). All bars represent the mean ± SE of at least three experiments (A, B, E and F).